International Journal of Civil, Structural, Environmental and Infrastructure Engineering Research and Development (IJCSEIERD)
ISSN(P): 2249-6866; ISSN(E): 2249-7978
Vol. 6, Issue 4, Aug 2016, 1-10

TRANS STELLAR
•Journal Publications •Research Consultancy

EFFECTS OF CONSTRUCTION JOINTS AND AXIAL LOADS ON SLIP BEHAVIOR OF RC SHEAR WALLS

RADORAMAROZATOVO[1], JUN HOSONO[2], TAISHIKAWAI[3], SUSUMUTAKAHASHI[4] & TOSHIKATSU ICHINOSE[5]

[1]*Research Student, Nagoya Institute of Technology, Nagoya, Japan*

[2]*Graduate Student, Nagoya Institute of Technology, Nagoya, Japan*

[3]*Undergraduate Student, Nagoya Institute of Technology, Nagoya, Japan*

[4]*Assistant Professor, Nagoya Institute of Technology, Nagoya, Japan*

[5] *Professor, Nagoya Institute of Technology Nagoya, Japan*

ABSTRACT

This research paper is an analysis of an experiment conducted on four RC shear wall specimens. The tested specimens were built with same dimensions, but taking different variables, such as the use of construction joint and the application of axial loads. The main purpose of the research was to determine the relationship between axial loads, construction joints and slip behavior of each specimen when put under an earthquake simulating cyclic shear load. The results of the experiment allowed concluding that specimens built with construction joint slip and fail after reaching maximum moment strength, as the vertical bars of the web get cut. On the other hand, slip is negligible in monolithic specimen and the failure of the specimen occurs on concrete, rather than on reinforcement. The results also enlightened how the increase of axial load affects the reduction of the width of cracks, the increase of strength of the specimen and its capacity to dissipate energy.

KEYWORDS: Slip, Shear Wall, Axial Load, Construction Joint

Received: May 28, 2016; **Accepted:** Jun 13, 2016; **Published:** Jun 20, 2016; **Paper Id.:** IJCSEIERDAUG20161

Original Article

INTRODUCTION

Regarding seismic issues on RC walls, codes such as ACI or Eurocodes take in consideration the slip at the same level as shear or bending strength at design. To understand the slip behavior, its impact on the strength and the stiffness in a squat RC wall, it is rather important to investigate and predict the behavior of the structure. For that purpose, four wall specimens nearly identical with a span ratio of 0.56, are built, axially loaded and subjected to a horizontal shear force. The applied load is a reversed cyclic one, which simulates the effect of an earthquake. Design codes such as ACI and Euro code are used to predict the slip strength of the specimen.

EXPERIMENT

Specimens

Four reinforced concrete wall specimens with the dimensions specified in Figure 2 are built to conduct the study. Scaled at 1/2.5, three of the four specimens are different from one another by the intensity of axial load applied at the top of each one. The values of the axial loads are specified in Table 1. The specimens are separately cast from their bottom supports creating construction joints between the walls and the bottom supports.

The construction joint is obtained by applying an Acrylic Resin Emulsion. The fourth specimen differs from the three by the absence of construction joint, making the bottom support and the wall monolithic.

The reinforcements of the web for all specimens are D4@80mm for vertical bars and D4@50mm for horizontal bars. Two boundaries are integrated in each specimen with 6D10 as main reinforcements, confined with D4@50mm ties. The reinforcements are designed with Japanese standard (Ref. AIJ, 2003) and detailed in Table 2 and Figures 1 and 2.

Table 1: Parameters of the Specimens

Specimen	Construction Joint	Axial Stress
J-N0	Yes	0 N/mm2
J-N1		1 N/mm2 (223kN)
J-N2		2 N/mm2 (446kN)
M-N2	No	

Table 2: Reinforcements of Specimens

	Sections (mm)	Reinforcements	
		Vertical	Horizontal/ties
Web	1860x120 (H=1050)	17D4@80 (ρ_{wg}= 0.29%)	20D4@50 (ρ_{ww}= 0.47)
Boundaries	240x120	6D10 (ρ_{cg}= 1.49%)	20D4@50 (ρ_{cw}= 0.47)

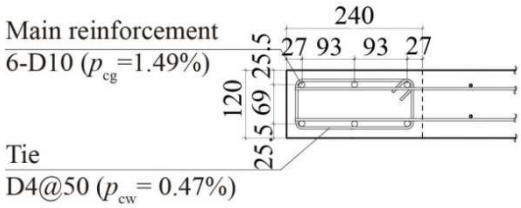

Figure 1: Reinforcement of the Boundaries

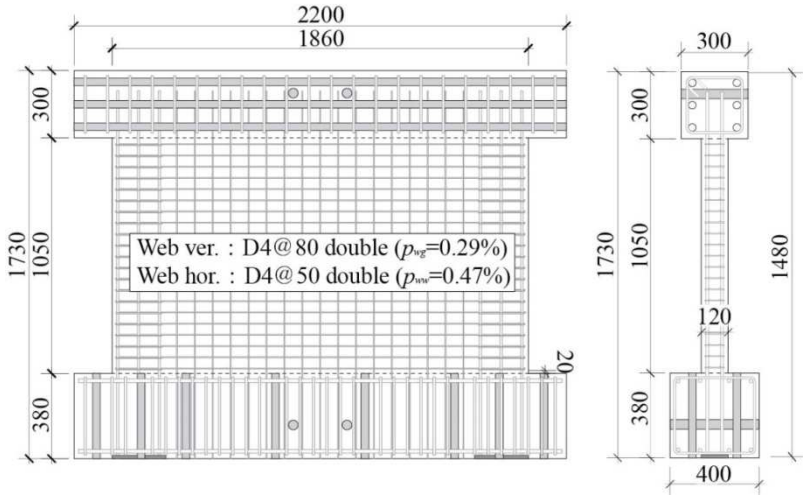

Figure 2: Dimensions and Reinforcements of the Specimens

Considering that Japanese code does not consider slip at the designing process, ACI318, Eurocodes and T. Pauley's formulas are used to verify the slipping capacity of the specimens. The formulas, despite their different origins, have the same components: The dowel action of the vertical reinforcements and the friction resistance of the construction joint. The slip of specimen was predicted as the computed slip strengths gave smaller values than shear strengths. Calculated values are shown with test results later.

The shear strength was computed using Japanese code (Ref. AIJ, 2010)

$$Qsu = \left\{ \frac{0.068 Pte^{0.23}(F_c+18)}{\sqrt{\frac{M}{Q \cdot D}+0.12}} + 0.85\sqrt{\sigma_{wh} \cdot p_{wh}} + 0.1\sigma_0 \right\} t_e \cdot j \quad (1)$$

F_c: Compressive strength of concrete	σ_{wh}: Yield strength of shear reinforcement
j: Stress center-to-center distance	σ_0: Average axis stress
$M/Q \cdot D$: Shear-span ratio	t_e: Thickness of the web
P_{te}: Tensile reinforcement ratio	
p_{wh}: Horizontal shear reinforcement ratio	

Loading Set-Up and Load Cycles

As shown in Figure 3, the axial load is applied with two center-hole hydraulic jacks placed on fixed steel plates on the rigid top stub of each specimen. At the two faces of the wall, the hydraulic jacks are attached to the bottom support with two ϕ26 PC bars. And in order to simulate the reversed cyclic load of an earthquake, two other hydraulic jacks are used to induce horizontal load at the top of the specimens, at a height of 1200mm from the upper bound of the bottom support.

The deformations are measured with strains gauges fixed on the reinforcements and with differential transducers.

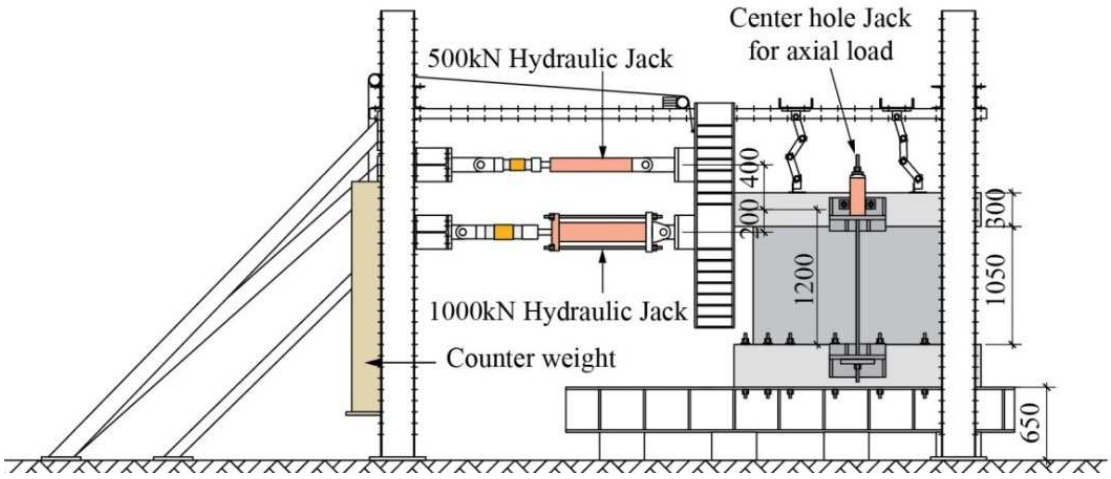

Figure 3: Loading Set-Up

Concerning the loading, the first two cycles of the experiment are defined by loads values: 90kN and 180kN. Those values represent the provisional calculated loads, before and after cracks appearance on the concrete. Thereafter, the cycles are defined by the following drifts of the top of the specimen: 0.15%, 0.30%, 0.45%, 1.0%, 2.0%, 3.0%, and 4.0%.

RESULTS AND INTERPRETATIONS

Failure Process

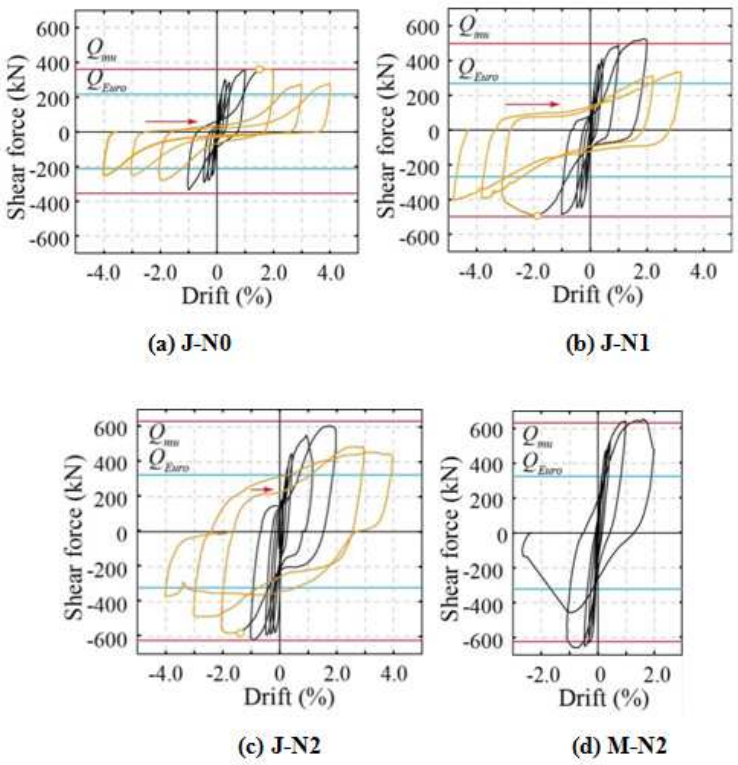

Figure 4: Shear Force - Drift Relationship

Figure 4 displays the shear force-drift of each specimen. The behavior of the specimen before any cut of reinforcements is represented by the black lines. During the loading in J-series, displacement is increased and cracks start appearing from 180kN cycle. After reaching the ultimate strength at 2.0% drift which corresponds to the computed ultimate moment strength, the reinforcements of the web start being cut. This phenomenon is followed by the loss of the strength of the specimen in the remaining cycles, represented in yellow lines. A difference can be observed regarding the drop of strength in J-N0 and J-N1 which is sudden at 2.0% drift, compared with that of J-N2 in whose drop occurs gradually until the end of the experiment. The reason of the drop of strength is explained in the next paragraph.

J-N1 specimen has been subjected to the dysfunction of the shear deformation measuring transducer at -2.0% cycle. Unable to do direct measure at -2.0%, the displacements were computed with the deformations ratio relationship:

$$\text{Slip} + \text{Moment} + \text{Shear} = 100\% \quad (2)$$

The obtained results caused the reduction of -1% of all displacements that occurred after -2.0% cycle, which allowed tracing Figure 4b.

In J-series specimens, the experiment ended with the cut of the vertical reinforcement of the web and the degradation of the concrete around the boundaries. The size of these degradations varies according to the specimen, as shown in Picture 1 and Figure 5. In the case of J-N2, in addition to the bars in the web, two vertical bars in the right boundary also got cut at -295kN load during the last –4.0% cycle. The absence of necking on the bars allows concluding that the cut is caused by shear failure. Picture2shows the vertical bars cut of the web and the boundary after the experiment.

The behavior of M-N2, compared with that of the J-series, stands out by its bigger flexural strength. Failure occurs at -2.0% cycle, when the concrete is sliced horizontally at about 1/3 height from the bottom support.

The comparison of the results from experiment and computation in Table 3 shows that the provisions about maximum flexural strength of each specimen agree with the experiment. Concerning the slip, though it is not the case of ACI formula, both Eurocodes and Paulay's formulas agree that slip occurs before the ultimate moment strength, which is in accordance with the results of the experiment.

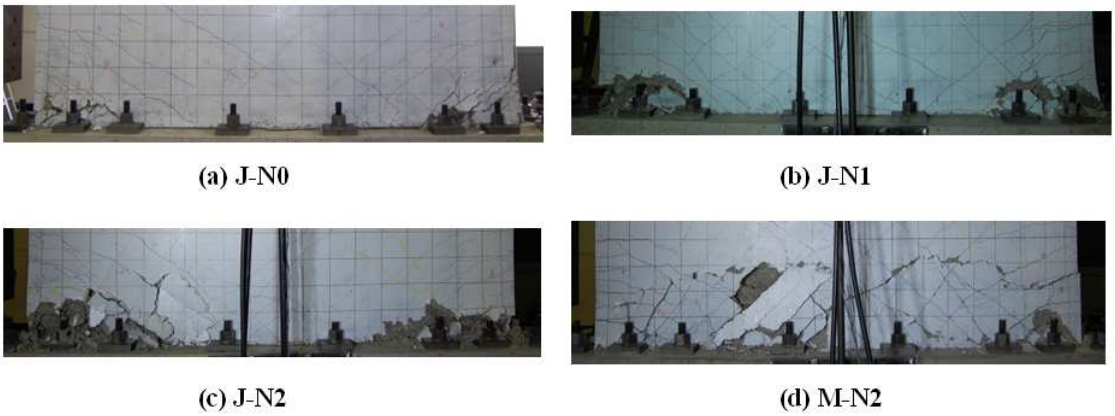

(a) J-N0 (b) J-N1

(c) J-N2 (d) M-N2

Picture 1: Degradation of Specimen at the End of the Experiment

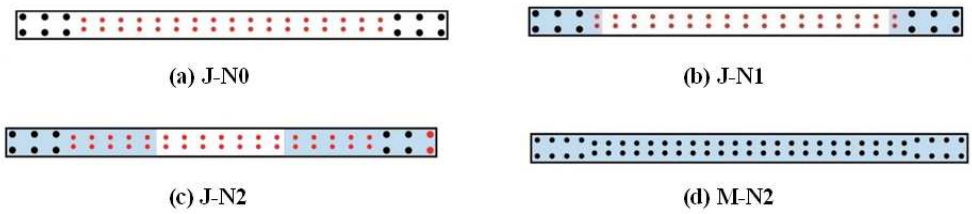

(a) J-N0 (b) J-N1

(c) J-N2 (d) M-N2

Figure 5: Location of Cut Bars and Damaged Area of Concrete

Picture 2: Vertical bars cut in J-N2

Table 3: Summary of Shear Strength and Shear Friction from Provisions and from Experiment

	Strength		Shear-Friction			Experiment Maximum Shear Force
	Flexure	Shear	ACI	Eurocode	Pauley	
	Q_{mu}	Q_{su}	$Q_{ACI} = V_n$	$Q_{Euro} = V_{rd.s}$	$Q_{Pau} = V_n$	
J-N0	363	538 (1.48)*	1020 (2.81)	220 (0.60)	112 (0.30)	360 (1.00)
J-N1	503	557 (1.11)		274 (0.54)	162 (0.32)	522 (1.04)

J-N2	632	575 (0.91)		328 (0.51)	225 (0.35)	628 (0.94)
M-N2			1323 (2.10)			666 (1.05)

*(): Ratio compared to flexural strength

Drop of Strength and Friction Coefficient

In J-N0, the cause of the loss of strength is the cut of the vertical reinforcements of the web. This statement is verified by computing the shear strength of the cut bars with the Von Mises criterion relation:

$$\tau_y = \sigma_y/\sqrt{3} \tag{3}$$

The value of the shear strength of the reinforcement of the web J-N0 is then:

$$T = 34\text{bars} \times 14\text{mm}^2 \times \frac{382\text{MPa}}{\sqrt{3}} = 105\text{kN} \tag{4}$$

That value corresponds to the drop obtained during the experiment displayed in Figure 6.Taking the case of J-N2 however, the loss of strength during the experiment is bigger. Among other possible reasons, it is caused not only by the cut of reinforcement, but also by the degradation of the concrete around the boundaries and whose size is as stated earlier, different depending on the specimen. In other words, the loss of strength depends on the intensity of the applied axial load.

Regarding the overall strength of the specimens, the friction also takes a non-negligible part. As indicated in the red ellipse in Figure 6, the resistance of J-N0 around zero drift is very small, indicating small friction at the construction joint. To discuss the phenomenon, Figure 7a shows the relationship between the drift and the uplift of the specimen at the center of the construction joint. As indicated in the blue ellipse in Figure 7a, the uplift around zero drift increases as the drift amplitude increases (Figure 7c). This increase is caused by the residual plastic strains in the vertical reinforcement. In J-N2 as well as in J-N1, however, the application of axial loads causes a bigger resistance of the specimens to uplift, as pointed in the blue ellipse in Figure 7a. Therefore, the reduction of the uplift causes the increase of friction within the construction joint.

It is not an easy task to compute the drop of friction throughout a specimen; however, it is possible to understand its variation within the different specimens. To compare the variation of friction, axial and shear stresses relationship is represented in positive and negative cycles at 2.0%, 3.0% and 4.0% in Figures 8a and 8b. Shear stress is defined by thes hear force divided by the horizontal section of the wall. The value of the shear force is taken at zero drift as indicated by the red points in Figure 8a, since at this stage; the dowel action does not take effect yet. The results in Figures 8a and 8b show that shear force increases along with the axial load. Moreover, the trend of the graphs, especially at 4%, is closely similar to the slope of the tangent of Mohr circles (μ =0.75), indicated by the broken lines, which represents the friction coefficient. This comparison allows understanding that the friction is a variable that depends on the intensity of the axial stress.

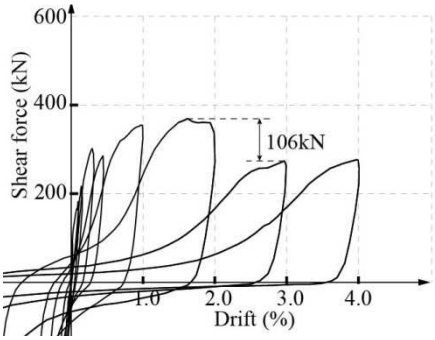

Figure 6: Drop of Strength in J-N0

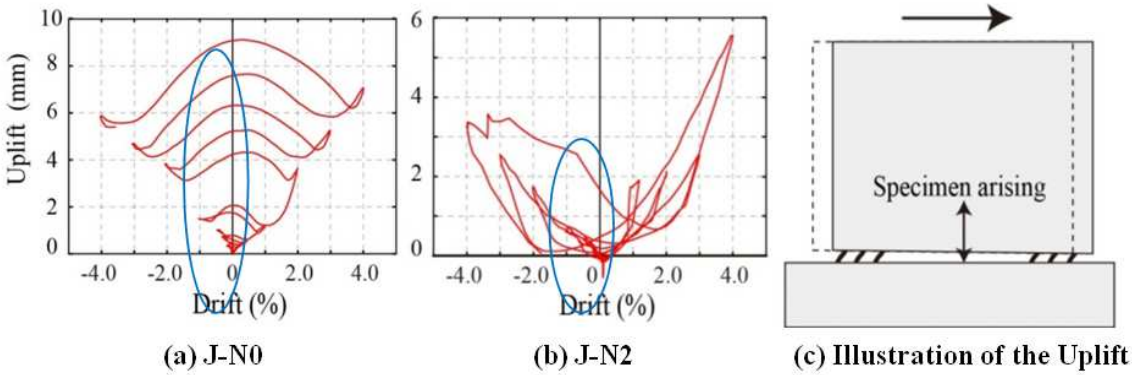

Figure 7: Uplift of Specimens during Experiment

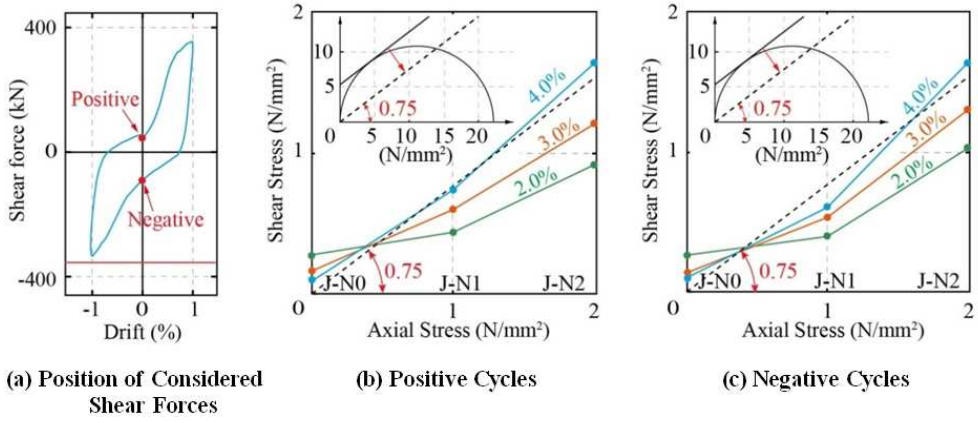

Figure 8: Variation of the Friction Coefficient

Cracks Patterns

Figure 9 compares the crack patterns of the specimens. The patterns in J-Series shows distinctive shear cracks and flexural cracks. Most of the shear cracks do not reach the compressive zone. Regarding the widths at 1.0% cycle, as represented in millimetre in Figure 9, axially loaded specimens J-N1 and J-N2 show smaller gaps, but the widest cracks are observed in M-N2. The cracks in the monolithic specimen are widely spread over the web and the boundaries. Moreover, flexural and shear cracks are joined and reach the bottom support in both the flexural tensile and compression zone. The low capacity of the specimen to slip caused the deformations to be focused on shear and flexure; but the excessive spread of cracks weakened the section of the concrete and ultimately leads to its failure.

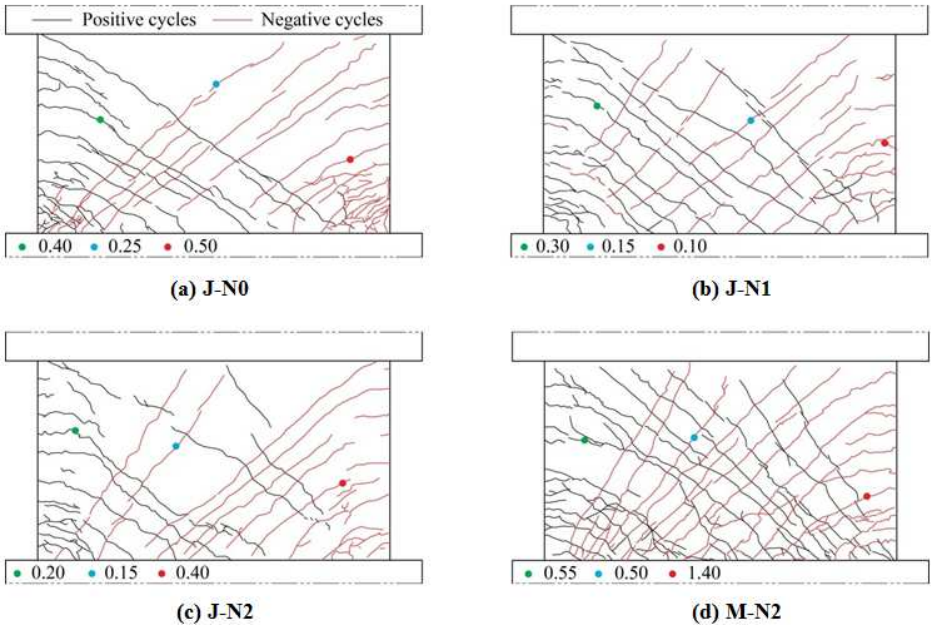

Figure 9: Cracks Patterns and Comparison of Widths of Cracks in Mm At 1.0% Cycle

Slip Deformation

It is noted that slip deformation displayed in Figures 10a, 10b and 10cis about 1% smaller than the drifts in Figures 4, in the jointed specimens. Also, the incapacity of the monolithic specimen to slip is translated by the slim shape of the graph in Figure 10d. The shapes of the hysteretic responses in Figures 4 and Figures 11 are similar in the J-Series, which means that slip deformation defines most of the deformations in the specimens.

This affirmation is supported by Figure 11 which displays the detailed ratios of moment, shear and slip deformations at the peaks of each cycle, in each specimen. The blue lines represent the moment deformation ratios and the red lines, the sum of moment and shear deformation ratios. In J-series, the red curves tend to point to 100% at 0% deformation, meaning than the deformations at the initial cycles are caused by shear and moment only. As the cycles continue, the slip areas increases, which implies the increase of slip deformations. Between J-N1 and J-N2, no major differences can be remarked; however, the capacity of J-N0 to slip is bigger, especially during the positive initial cycles.

Finally, regarding M-N2's diagram, the small slip area likewise confirms that slip is negligible compared to the flexural and shear deformations. In opposite with M-N2 of the present experiment, considerable amount of slip was observed in a monolithic specimen in similar previous experiment conducted on RC shear walls without axial load (Ref. HOSONO Jun, 2015). It was however noted that the ratio of slip of that monolithic specimen was smaller than that of a specimen with construction joint. That comparison allows concluding that the application of axial load is a variable that prevent or reduce slip in a monolithic specimen.

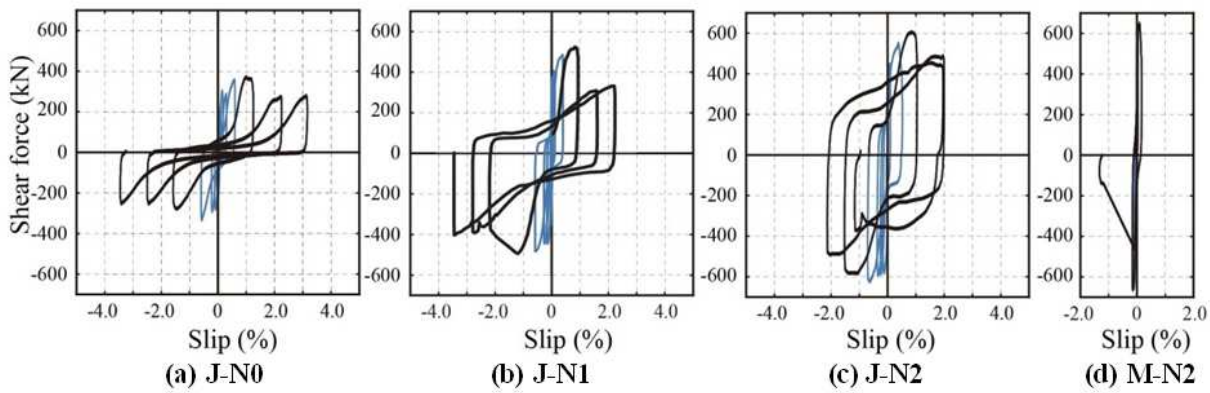

Figure 10: Shear Force - Slip Relationship

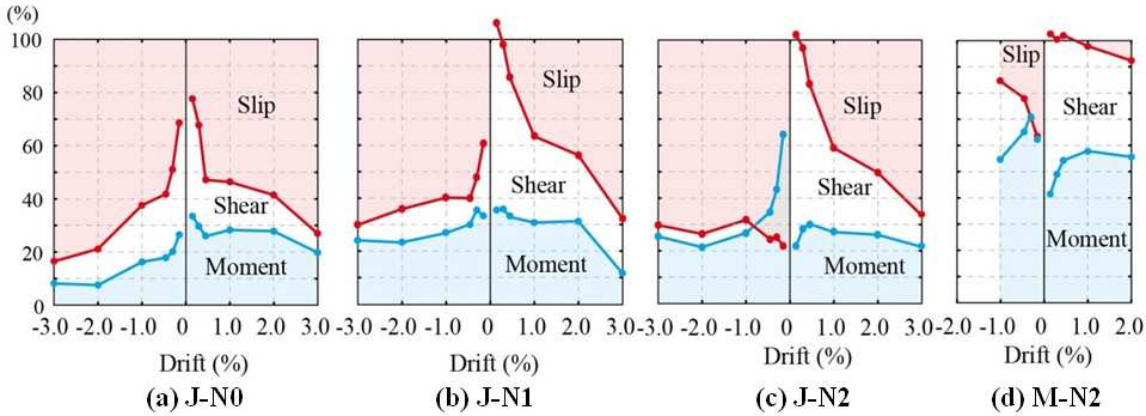

Figure 11: Ratios of Deformations at Cycles

Energy Dissipation

The comparison of the hysteretic behaviors of the J-series as in Figure 10 shows that the amplitude of the shear force is increased at slip equals zero, as so as the axial load. This variation of the amplitude translates the capacity of a specimen to dissipate energy. The energy dissipation is the value of the area enclosed within the load - displacement curve shown in Figure 12a. To neglect the difference of flexural strengths Q_{mu} and displacement amplitude$\Delta\delta$in each specimen, the rate of the energy was computed by dividing the energy by $Q_{mu}.\Delta\delta$, the area of the blue rectangles in Figure 12a. The results of such computation at 1.0% and 3.0% cycles are illustrated in Figure 12b. The graph in J-series tends to increase with the increase of axial load. Regarding M-N2, its energy dissipation is smaller of that of J-N2 at 1.0% cycle, which may confirm one of T. Pauley's conclusion which states that the sliding shear along the base is the main cause of reduction of the ability of a specimen to dissipate energy, unless the specimen is subjected to a high axial loading or special conditions (Ref. T.Paulay, 1982).

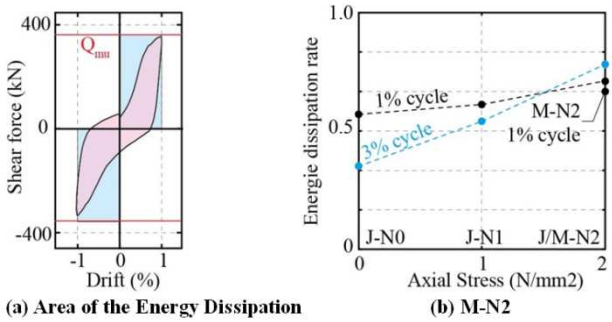

Figure 12: Variation of Energy Dissipation

CONCLUSIONS

The results from the experiment set up to investigate about the effects of axial loads and construction joint on the slipping behavior of four RC shear walls specimen led to the following conclusions:

- In specimens with Acrylic Resin Emulsion construction joint, the experiment ends with all the vertical reinforcement in the web cut after reaching maximum moment strength.
- In monolithic specimen, slip is negligible and the failure of concrete is reached before any cut of reinforcement. The absence of slip in the monolithic specimen proves that the existence of construction joint is the factor of slip in an axially loaded shear walls.
- In sliding specimen, the increase of energy dissipation is proportional to the increase of the axial load on shear wall. However, based on the comparison with a monolithic specimen, slip is not a factor that reduces the capacity to dissipate energy.
- The shear force at zero displacement during cyclic loading increases linearly depending on the increase of the intensity of axial load. The relationship between the shear force and the axial load is represented by a friction coefficient of 0.75.

REFERENCES

1. *American Concrete Institute, "Building Code Requirements for Structural Concrete Structures", ACI 318-11, 2011*
2. *James K. Wight and James G. MacGregor, "Reinforced concrete mechanics and design", 6th ed., Pearson, 2012.*
3. *Eurocode 8: Design of structures for earthquake resistance, Part 1: General rules, seismic actions and rules for buildings, British Standards EN (1998-1), 2004*
4. *Recommendation for Detailing and Placing of Concrete Reinforcement, Architectural Institute of Japan, 2003*
5. *AIJ Standard for Structural Calculation of Reinforced Concrete Structures, Architectural Institute of Japan, 2010*
6. *T.Paulay M.J. Priesley and A.J.Synge, Ductility in Earthquake Resisting Squat Shearwalls, ACI journal, Vol. 79, No.26, pp. 257-269, 1982*
7. *HOSONO Jun, Effect of Construction Joint and Bar Arrangement of Bar on the Slip Behavior of RC Shear Walls, Proceedings of the Japan Concrete Institute,Vol.36, No. 2, pp.355-360,2015*